

Closing the circle: d-wave order parameter symmetry in the electron-doped $Sr_{1-x}La_xCuO_2$ superconductors

Victor Leca

National Institute for Research and Development in Microtechnologies, Bucharest, Romania

*Present work address:
Extreme Light Infrastructure-Nuclear Physics (ELI-NP), Bucharest, Romania

Collaborators

Prof. Dieter Koelle, Univ. Tübingen

Prof. Reinhold Kleiner, Univ. Tübingen

Dr. Jochen Tomaschko, (former at) Univ. Tübingen

Prof. Dave Blank, Univ. Twente

Prof. Guus Rijnders, Univ. Twente

Dr. Mihai Danila, IMT Bucharest

Dr. Di Wang, Karlsruhe Institute of Technology

Dr. Wim Arnold Bik, AccTec BV, Technical Univ. Eindhoven

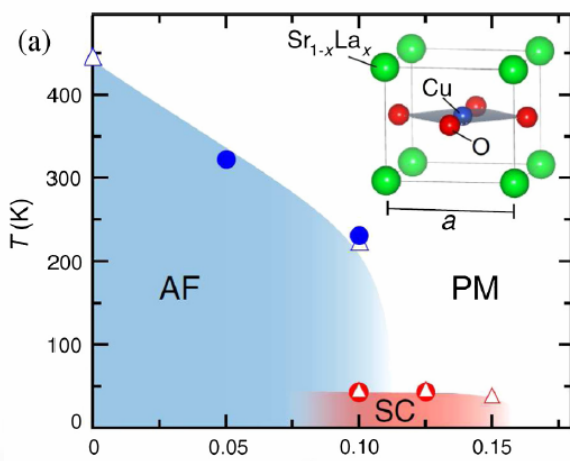
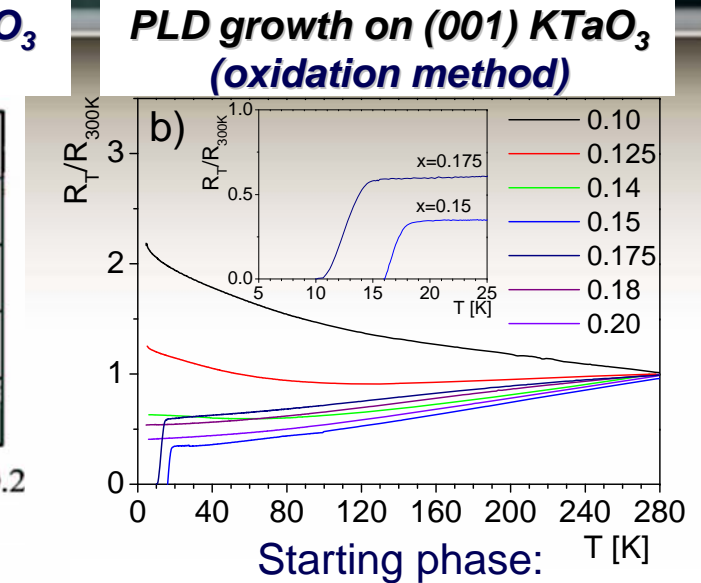
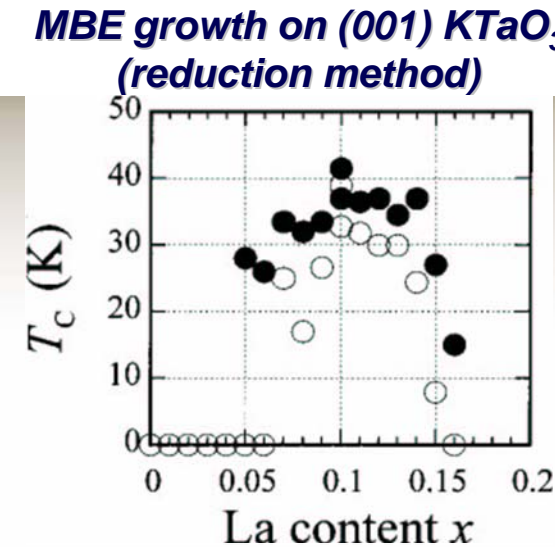
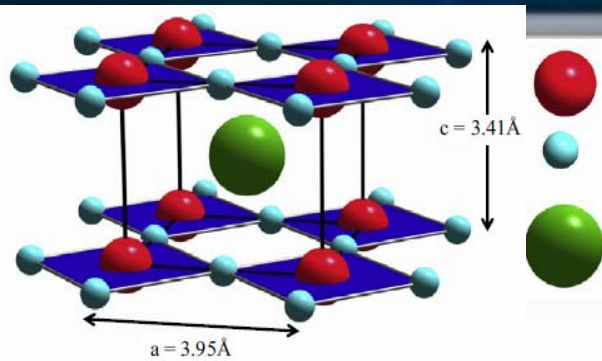
Acknowledgements

Deutsche Forschungsgemeinschaft (project KL 930/11)

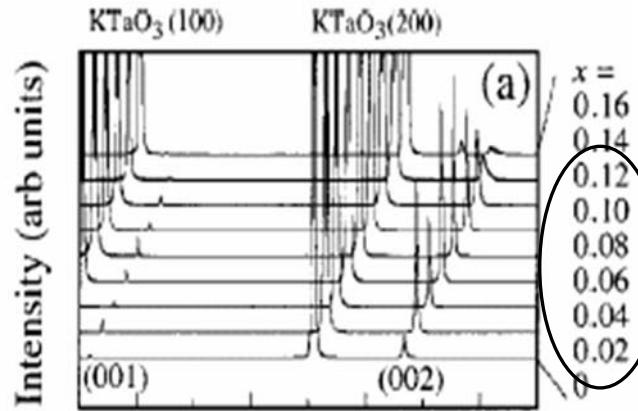
Romanian National Authority for Scientific Research, CNCS UEFISCDI,
project number PNII-ID-PCE-2011-3-1065

European Commission under the FP7 Capacities programme
(EUMINAFab project number 1090)

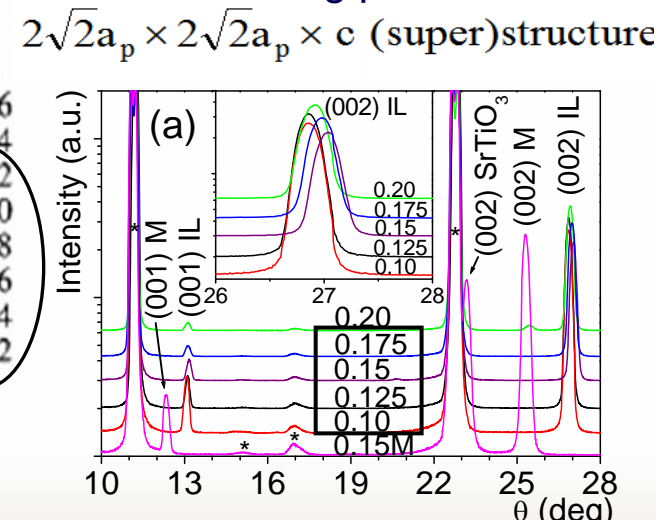
The $\text{Sr}_{1-x}\text{La}_x\text{CuO}_2$ (SLCO) compounds



T_c vs. dopant concentration phase diagram for bulk $\text{Sr}_{1-x}\text{La}_x\text{CuO}_2$



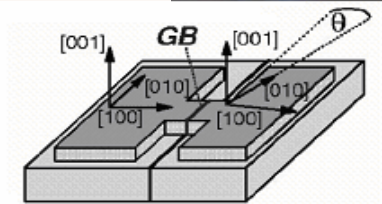
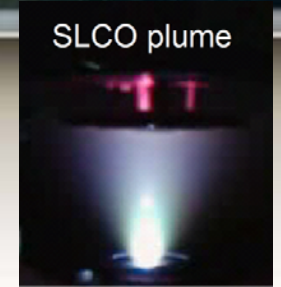
Karimoto et al. (APL 79, 2001)



Leca et al. (APL 89, 2006)

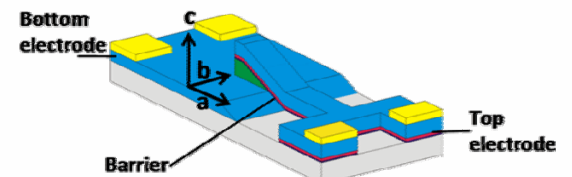
Outline

1. Correlation between strain, microstructure, and electrical transport properties in $Sr_{1-x}La_xCuO_2$ (SLCO, $x=0.10-0.175$) **thin films** grown by PLD on different substrates ($KTaO_3$, $SrTiO_3$, and $DyScO_3$)



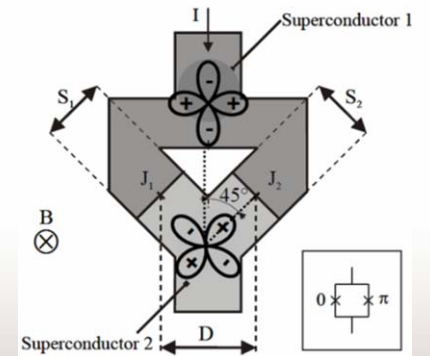
2. $Sr_{1-x}La_xCuO_2$ ($x=0.125-0.15$) **Josephson junctions**:

- grain-boundary junctions based on c-axis oriented films
- ramp-type SLCO/Au/Nb junctions



3. **Order parameter symmetry** – phase sensitive tunneling experiments based on $0/\pi$ -SQUIDs (on $SrTiO_3$ tetracryystals)

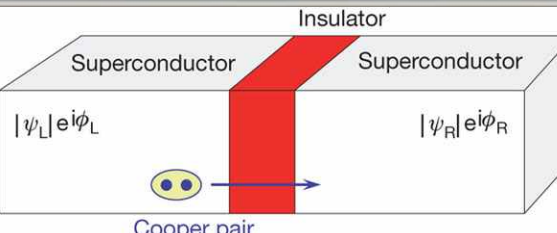
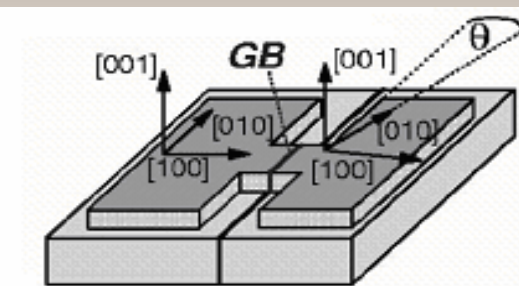
Is d-wave symmetry inherent to cuprate superconductivity?



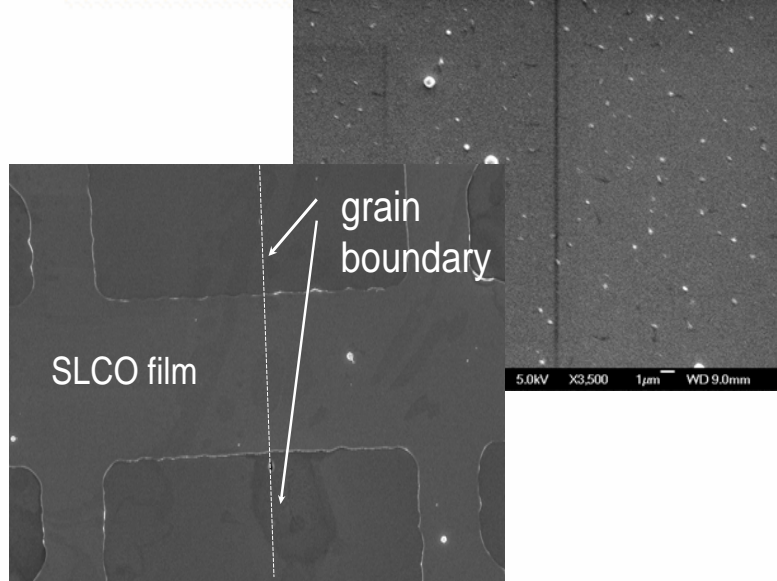
Thin films: growth and properties

Requirements for $\text{Sr}_{1-x}\text{La}_x\text{CuO}_2$ -based junctions

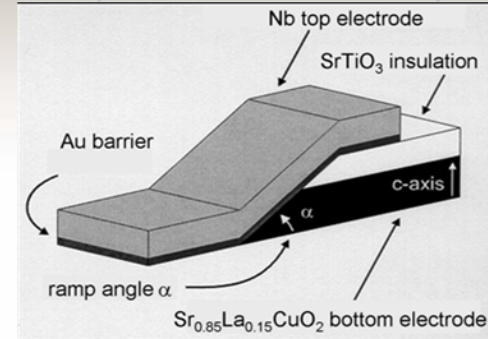
Grain-boundary



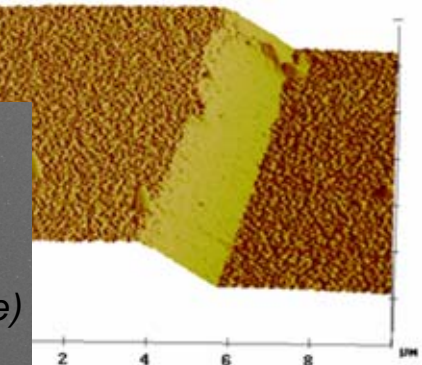
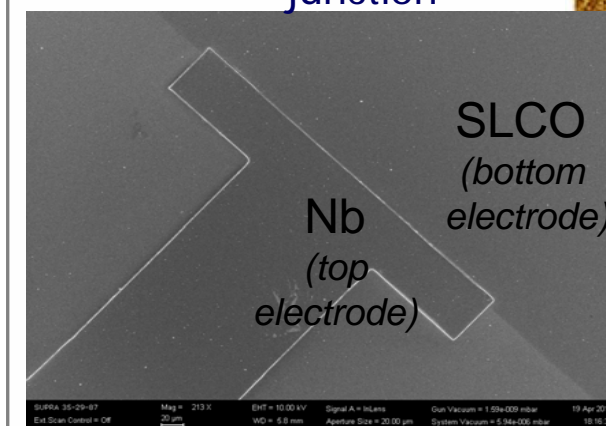
Josephson junction



Ramp-type ($\text{SrLaCuO}/\text{Au}/\text{Nb}$)



AFM of a ramp-type junction



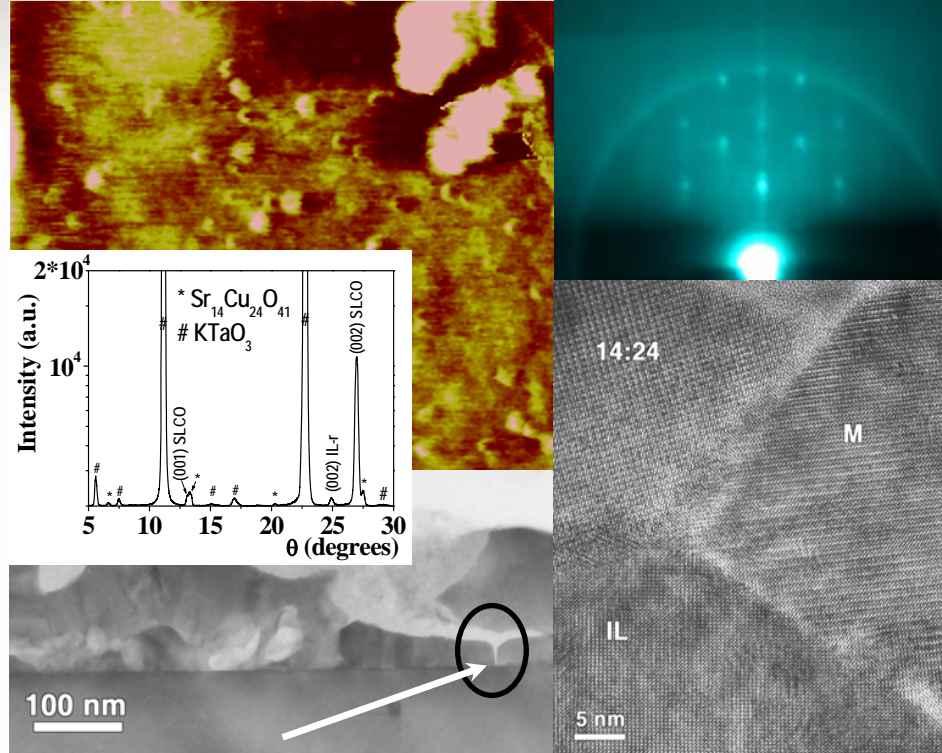
SEM of a 200 μm wide junction

Single phase, c-axis oriented films required

Single phase, c-axis oriented SLCO films, with smooth surface and sharp oxide-metal interface required

Role of the substrate-film interface (oxidation method)

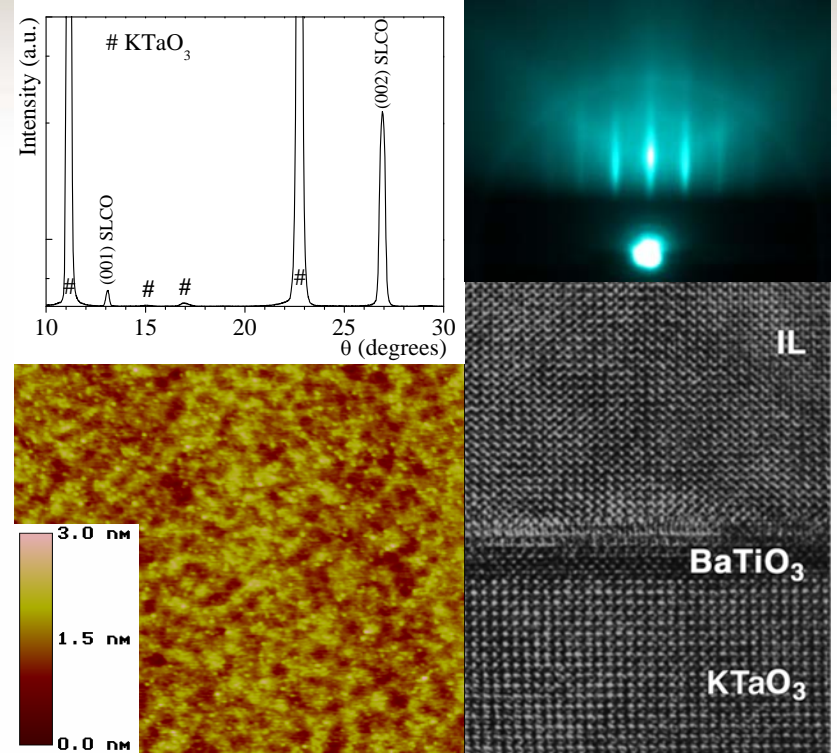
$\text{Sr}_{1-x}\text{La}_x\text{CuO}_2$ grown on
as-received (001) KTaO_3



XRD, HRTEM: Structural defects/secondary phases developing at the substrate-film interface
RHEED, AFM: 3D growth mode induced by the high interface roughness

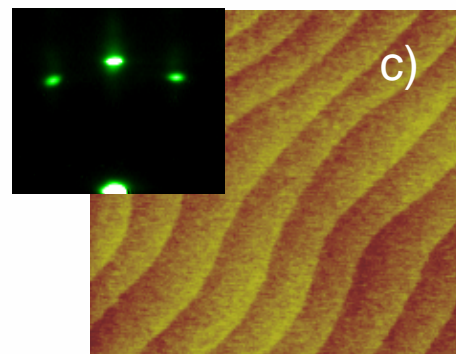
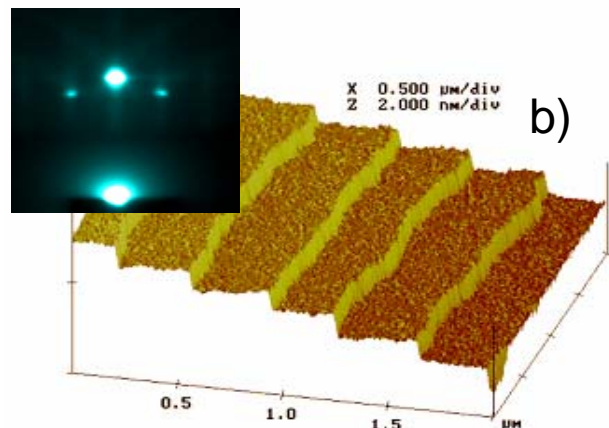
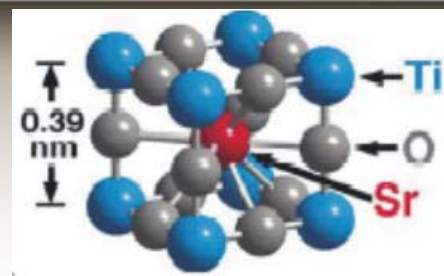
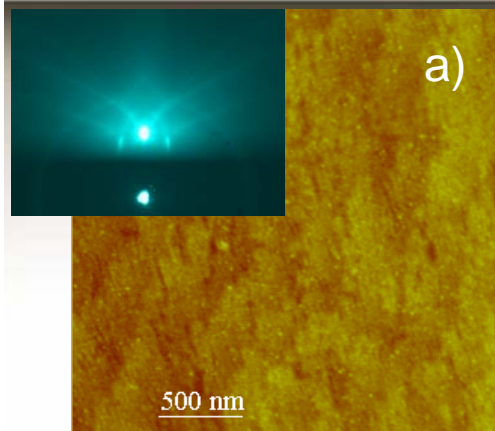
Leca, PhD thesis (2003), Leca et al. APL 89 (2006)

$\text{Sr}_{1-x}\text{La}_x\text{CuO}_2$ grown on
 BaTiO_3 -buffered (001) KTaO_3

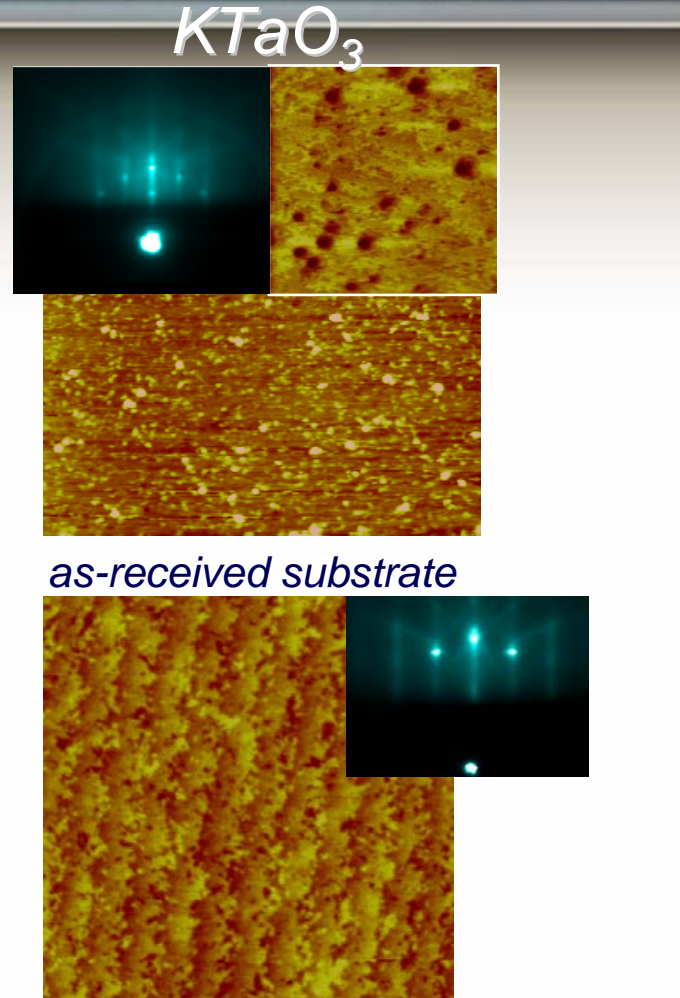


XRD, HRTEM, AFM: single-phase, reduced density of structural defects, improved morphology
RHEED, AFM: 2D growth mode

Improved substrate morphology – SrTiO₃ and KTaO₃



a) as-received substrate; b) after chemical treatment (BHF) and annealing (950°C/1h/O₂) - TiO₂ termination
c) after annealing (950°C/1h/O₂) - SrO termination



Kawasaki et al. Science 226 (1994); Koster et al. APL 73 (1998); Leca, PhD thesis (2003)

$\text{Sr}_{1-x}\text{La}_x\text{CuO}_2$ ($x \approx 0.15$) growth parameters

On (001) KTaO_3 and (110) DyScO_3

$\text{Sr}_{1-x}\text{La}_x\text{CuO}_2$ (SLCO):

$$T_d = 500-575 \text{ }^\circ\text{C}$$

$$P_d = 0.20-0.40 \text{ mbar O}_2$$

Post-deposition vacuum annealing (reduction) at T_d and 10^{-7} mbar:
- 10-20 min (KTaO_3 case)
- 20-30 min (DyScO_3 case)

T_c : up to 24 K, on KTaO_3
up to 18 K, on DyScO_3

Film's composition ($x_t=0.15$ target), from RBS data:

- $x_f = 0.145$, film grown on KTaO_3
- $x_f = 0.135$, film grown on DyScO_3

$$a_{\text{KTO}} = 3.988 \text{ \AA}, a_{\text{SLCO}} \sim 3.978 \text{ \AA}$$

$$a_{\text{DSO}(110)} = 3.944 \text{ \AA}, a_{\text{SLCO}} \sim 3.950 \text{ \AA}$$

On BaTiO_3 - buffered (001) SrTiO_3

BaTiO_3 (BTO):

$$T_d = 700-850 \text{ }^\circ\text{C}$$

$$P_d = 0.10 \text{ mbar O}_2$$

Post-deposition annealing:
- 15 min @ 950 $^\circ\text{C}$, under 0.10 mbar O_2 , and
30 min @ 950 $^\circ\text{C}$, in vacuum (10^{-7} mbar)

$\text{Sr}_{1-x}\text{La}_x\text{CuO}_2$ (SLCO):

$$T_d = 550-600 \text{ }^\circ\text{C}$$

$$P_d = 0.20 \text{ mbar O}_2$$

Post-deposition annealing (reduction):
45-60 min @ 550 $^\circ\text{C}$, in vacuum (10^{-7} mbar)

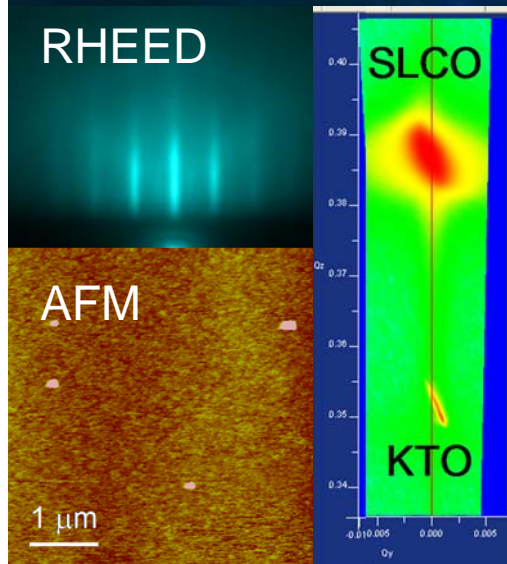
T_c : up to 21 K

Film's composition ($x_t = 0.15$ target), from RBS data: $x_f = 0.145$

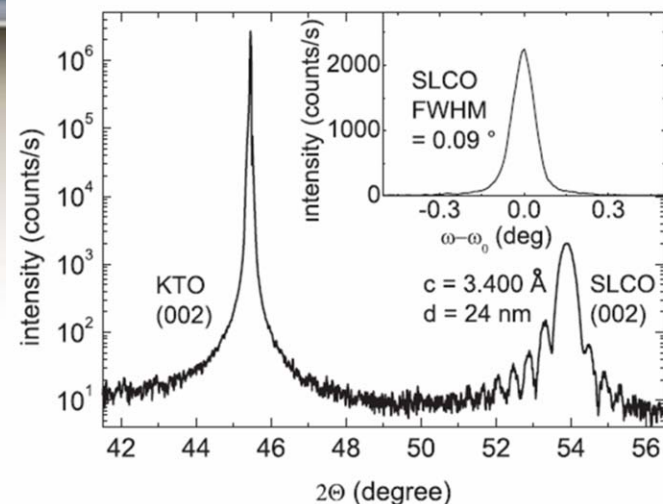
$$a_{\text{STO}} = 3.905 \text{ \AA}, a_{\text{BTO}} \sim 3.990 \text{ \AA}, a_{\text{SLCO}} \sim 3.967 \text{ \AA}$$

$Sr_{1-x}La_xCuO_2$ ($x=0.15$) grown on $KTaO_3$ (001)

RHEED



RHEED, AFM, and XRD rsm of (101) plane



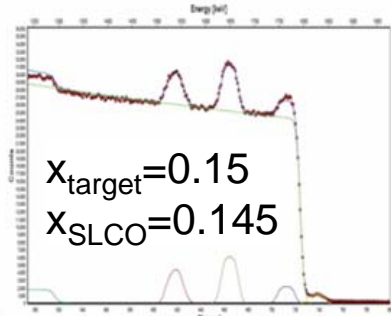
2θ/ω XRD scan of (002) SLCO/KTO

$$a_{SLCO} \sim 3.978-3.988 \text{ \AA}$$

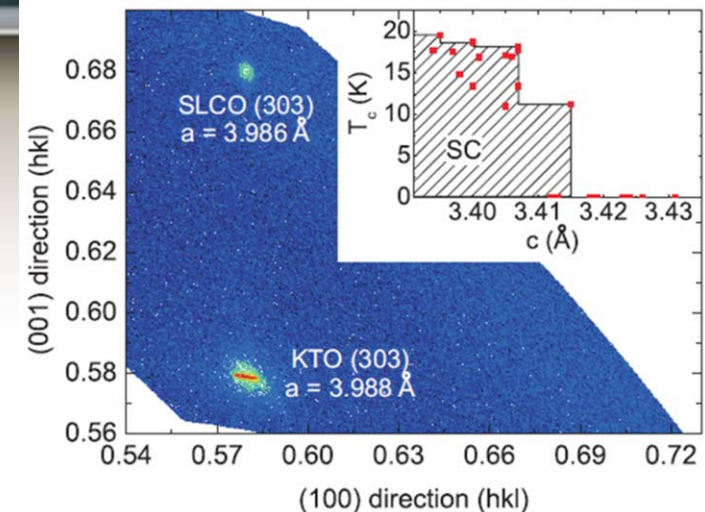
$$c_{SLCO} \sim 3.395-3.405 \text{ \AA}$$

Growth parameters:

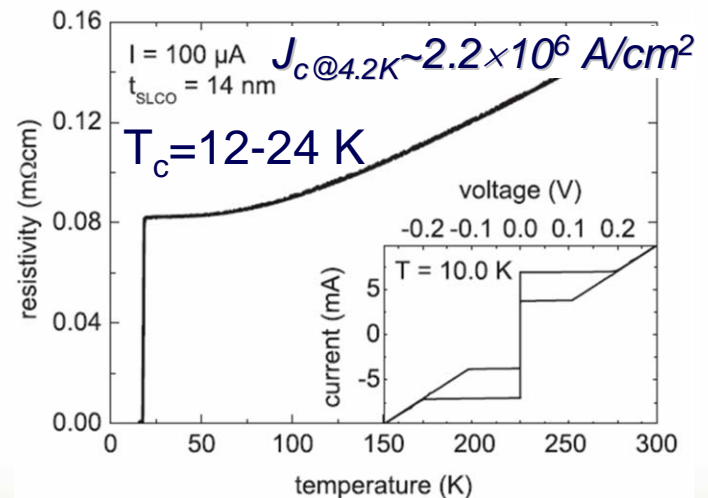
$Sr_{0.85}La_{0.15}CuO_2$ (SLCO): $T_d = 575^\circ\text{C}$,
 $P_d = 0.30 \text{ mbar O}_2$; $E_d = 2 \text{ J/cm}^2$;
20 min/550°C/10⁻⁷ mbar
films thickness: 15-50 nm.



RBS



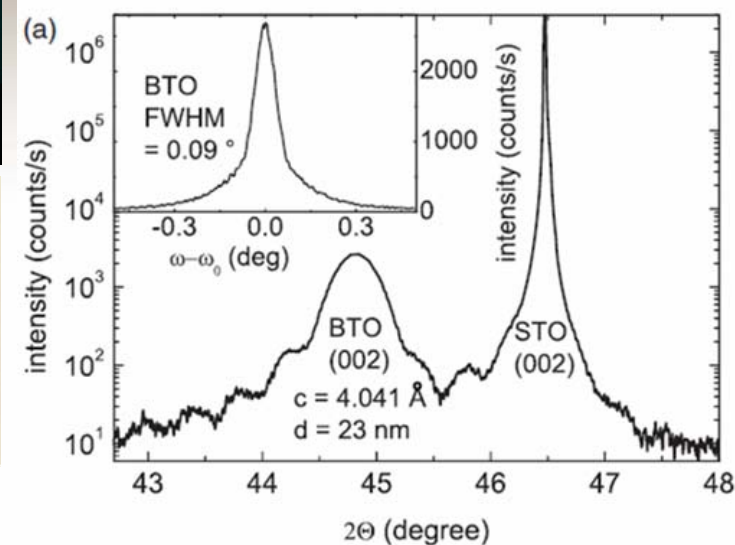
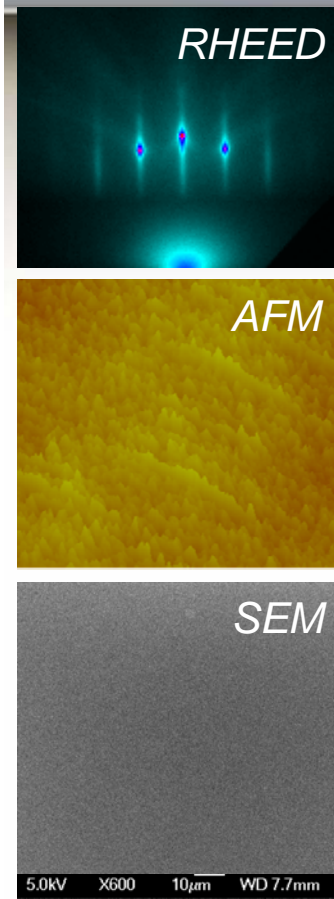
XRD reciprocal space map



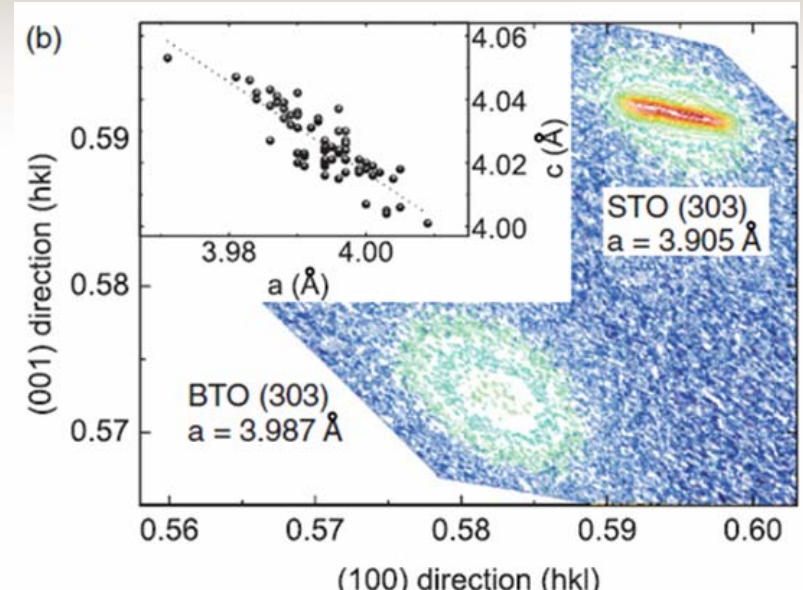
ρ vs. T

Tomaschko, Leca, Selistrovski, Diebold, Jochum, Kleiner, Koelle, Physical Review B 85 (2012)

$Sr_{1-x}La_xCuO_2$ ($x=0.15$) grown on $BaTiO_3/SrTiO_3$ (001)



The $BaTiO_3$ buffer layer

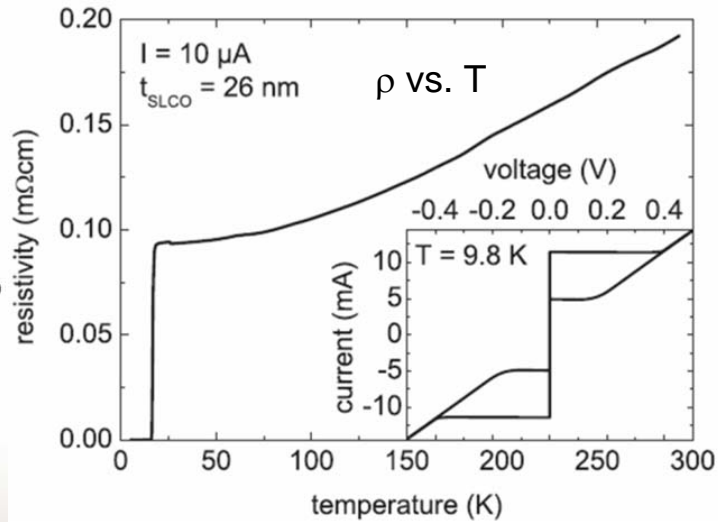
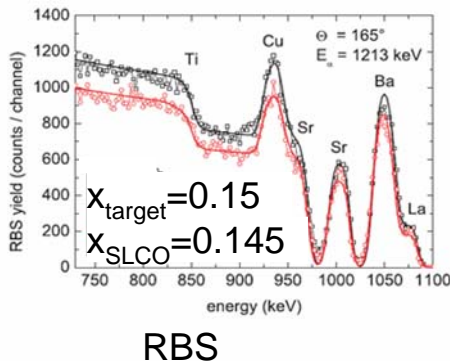
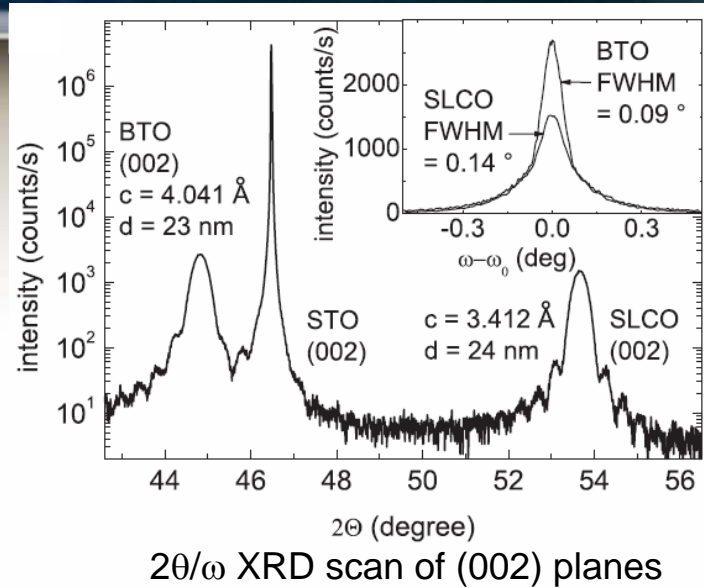
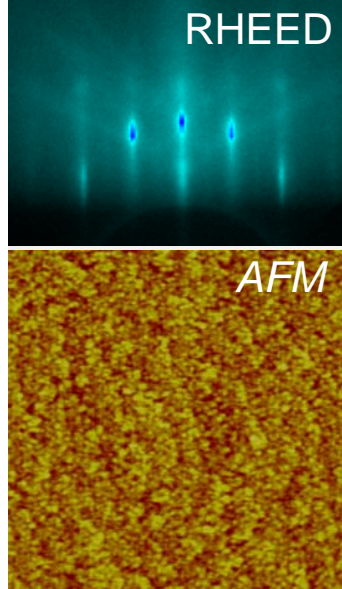


Deposition conditions for $BaTiO_3$:

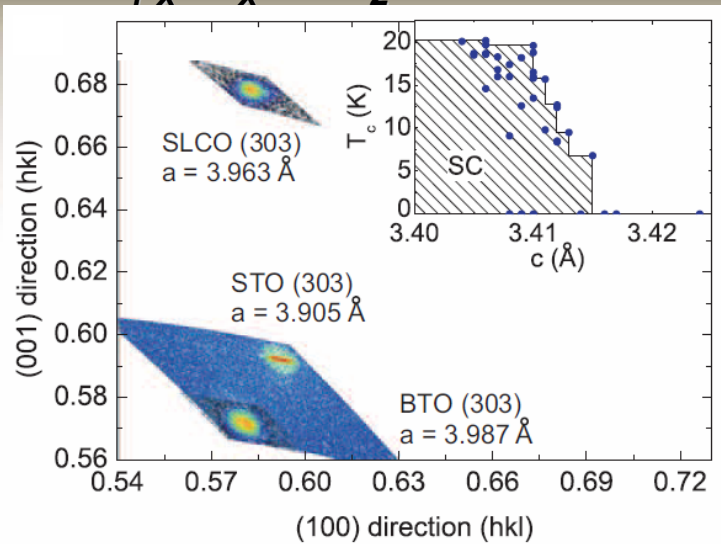
$T_d = 750^\circ C$, $P_d = 0.10$ mbar O_2 , $E_d = 1.75$ J/cm 2 ; 30 min/950°C/10 $^{-7}$ mbar

Tomaschko, Leca, Selistrovski, Diebold,
Jochum, Kleiner, Koelle, Phys. Rev. B 85 (2012)

$Sr_{1-x}La_xCuO_2$ ($x=0.15$) grown on $BaTiO_3/SrTiO_3$ (001)



$Sr_{1-x}La_xCuO_2$ films



XRD rsm of (303) SLCO/BTO/STO

Deposition conditions:

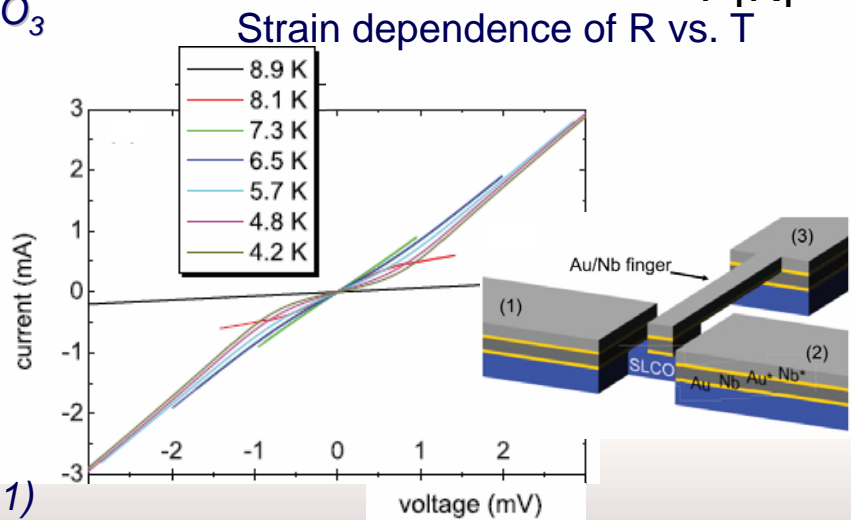
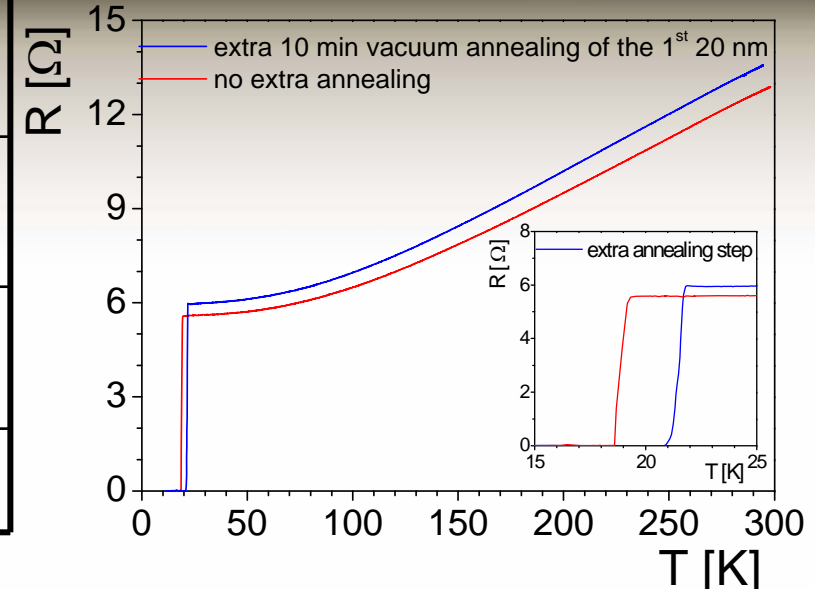
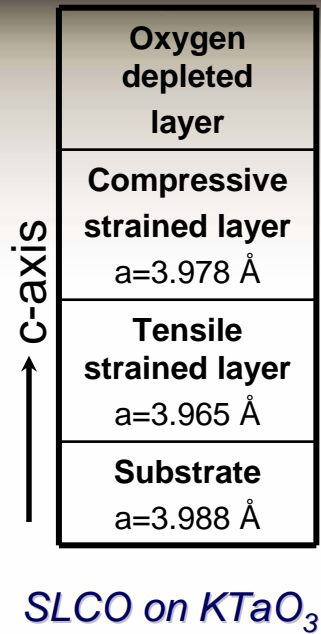
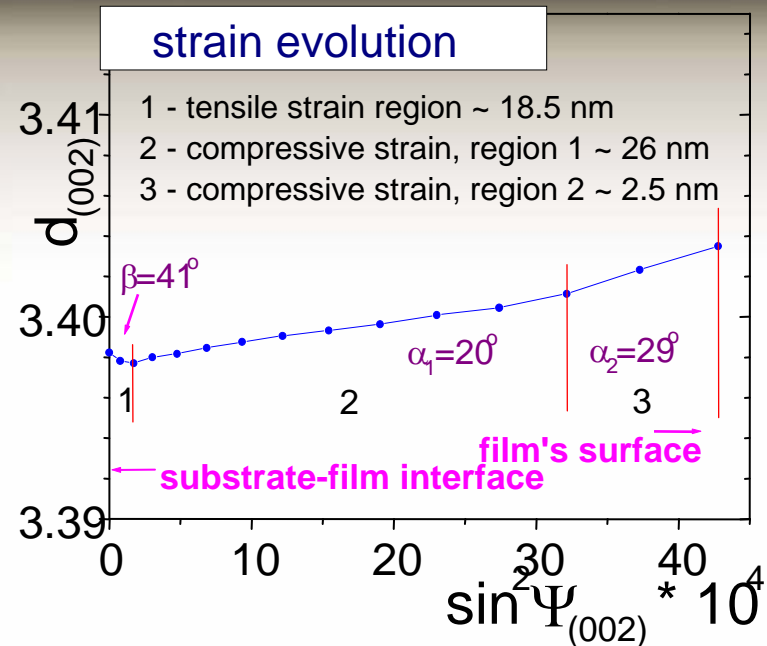
$T_d = 550^\circ\text{C}$, 0.40 mbar O_2 ;
50 min/550°C/ 10^{-7} mbar

$T_{c,0} = 12-21 \text{ K}$

$J_c @ 4.2 \text{ K} = 2.1 \times 10^6 \text{ A/cm}^2$

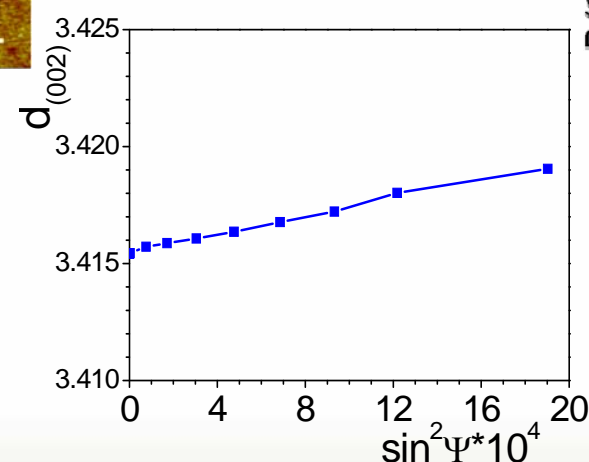
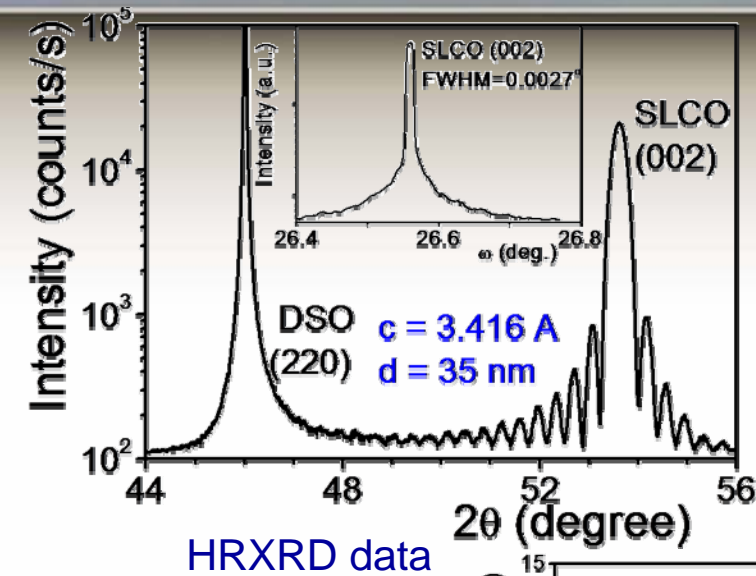
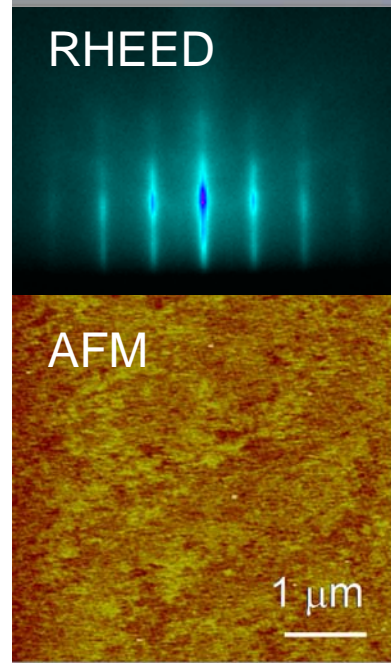
Tomaschko, Leca, Selistrovski, Diebold,
Jochum, Kleiner, Koelle, Phys. Rev. B 85 (2012)

Role of the epitaxial strain

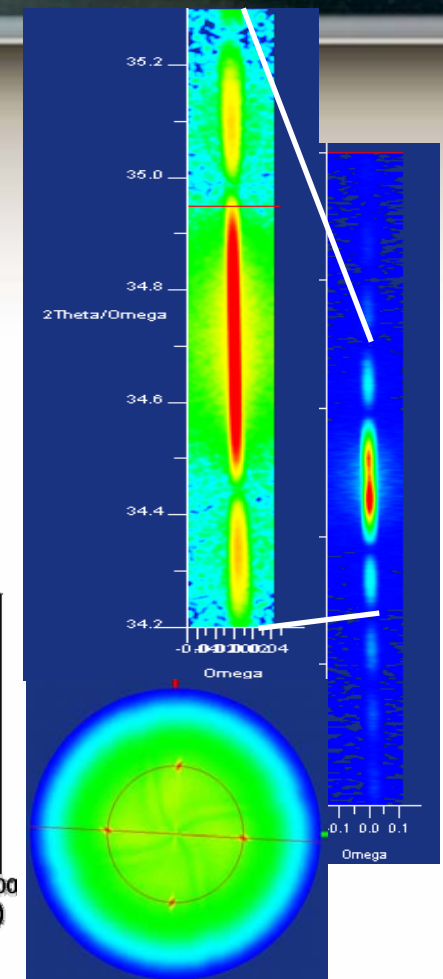
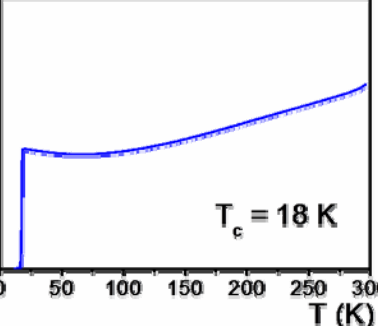


Tomaschko et al., PRB 84 (2011)

$\text{Sr}_{1-x}\text{La}_x\text{CuO}_2$ ($x \approx 0.15$) grown on DyScO_3 (110)

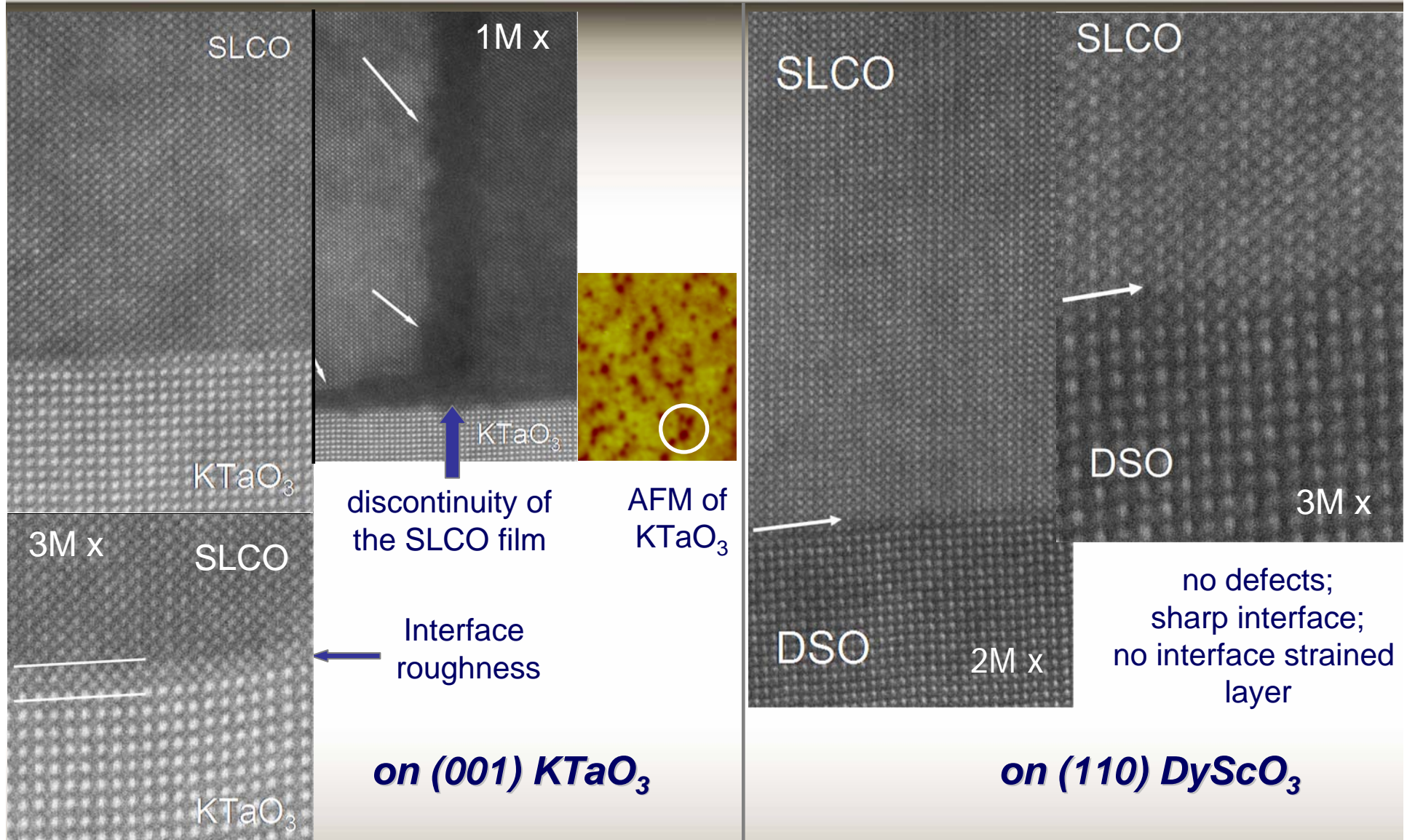


Strain evolution:
in-plane compressive strain

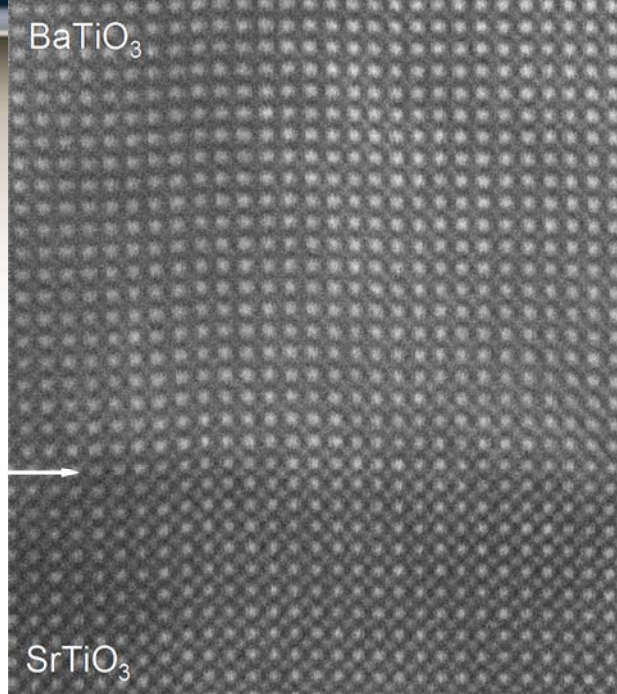


HRXRD rsm and pole figure
of the asymmetric (101) plane
Presence of Laue fringes
indicates high crystallinity

HRTEM results on $\text{Sr}_{1-x}\text{La}_x\text{CuO}_2$ ($x \approx 0.15$) film

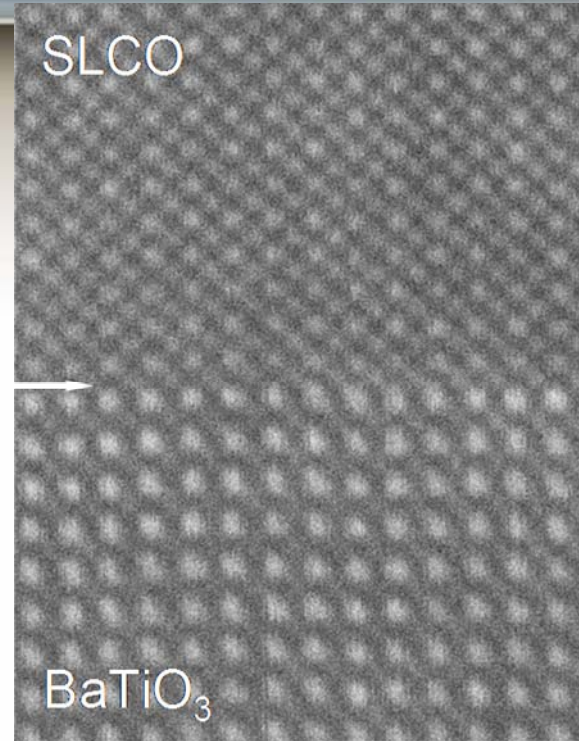


HRTEM results on $\text{Sr}_{1-x}\text{La}_x\text{CuO}_2$ ($x \approx 0.15$) film



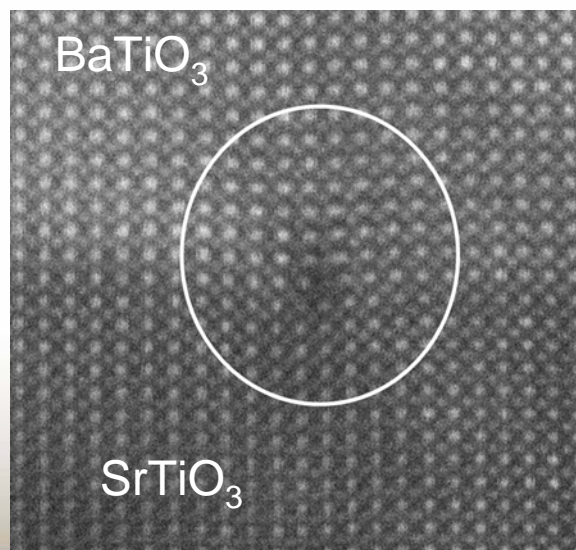
HRTEM

Sharp
interfaces



Sharp BTO-SLCO interface

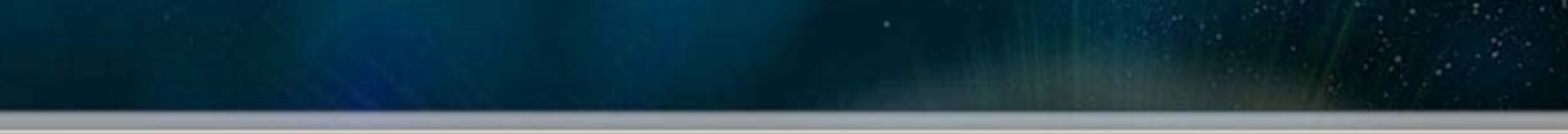
edge dislocation at the
STO/BTO interface



SLCO on $\text{BaTiO}_3/(001)$ SrTiO_3

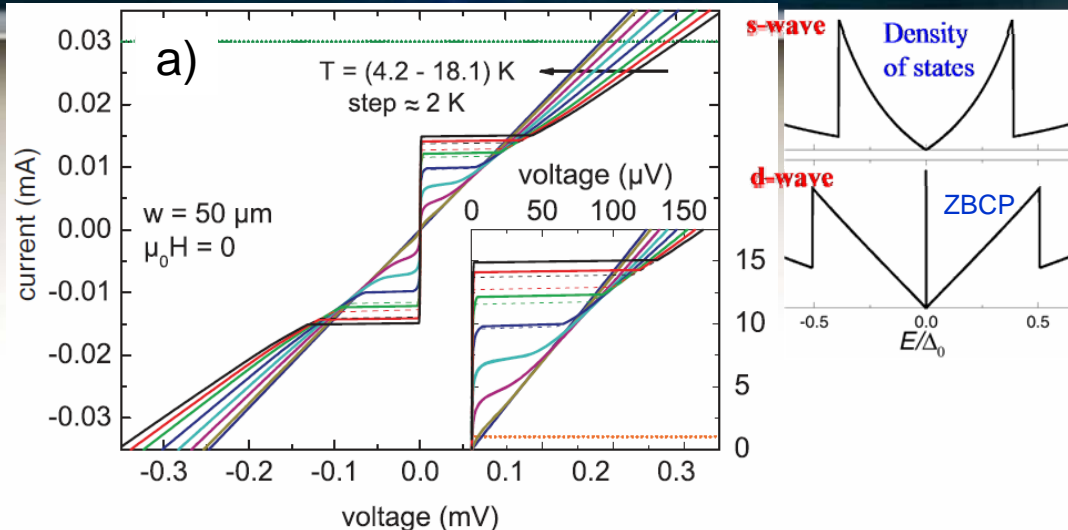
*Migration of the structural defects at the BTO/STO
interface due to high temperature annealing*

Terai et al., APL 80 (2002)



Josephson junctions: fabrication and transport properties

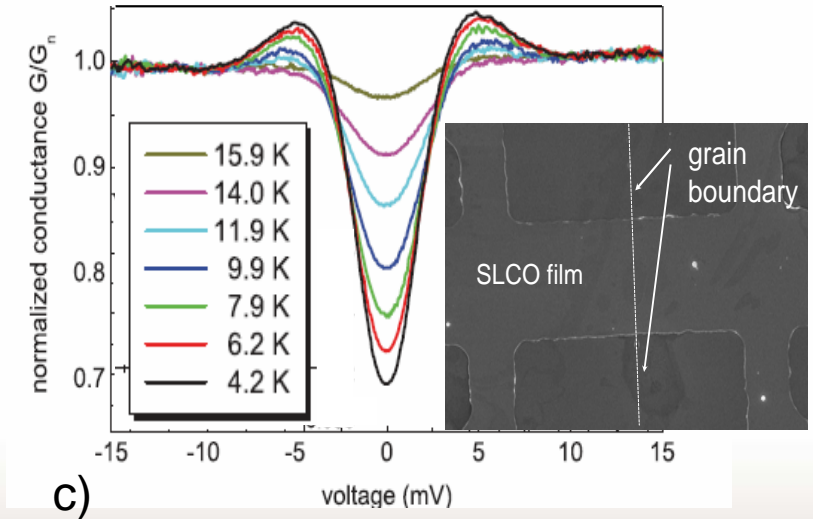
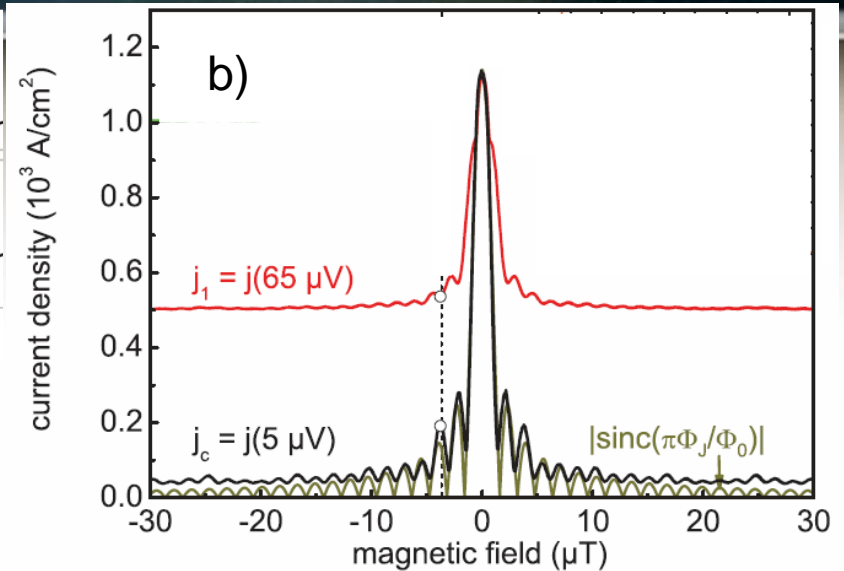
$Sr_{1-x}La_xCuO_2$ 24° symmetric grain boundary junctions



a) ICVs: resistively and capacitively shunted junction (RCSJ)-like, with no significant excess current;
- J_c (@ 4.2 K) $\sim 1.2 \text{ kA/cm}^2$ – 1-2 orders of magnitude above J_c of 24° GB based on NCCO and LCCO

b) highly regular Fraunhofer-like patterns for different voltage criterion

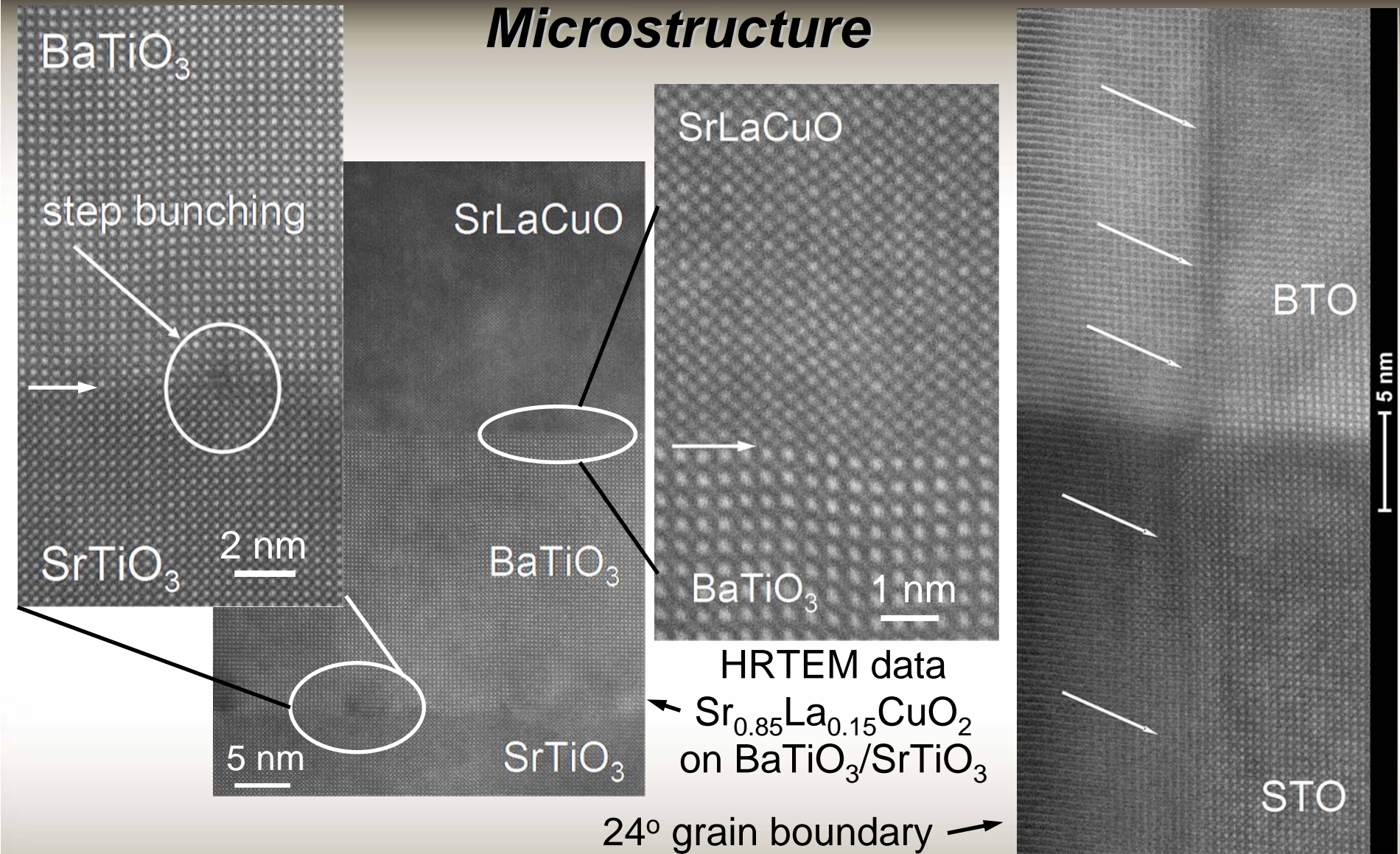
c) conductance spectra did not show a zero-bias conductance peak. s-wave symmetry?
but the V-shaped of the spectra in the subgap regime may indicate an order parameter with nodes



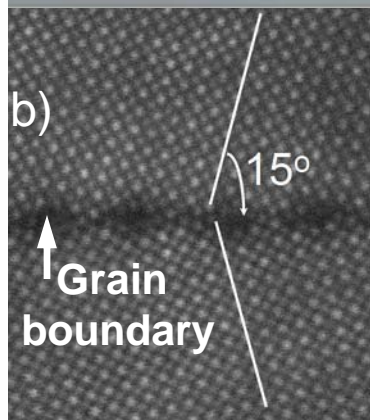
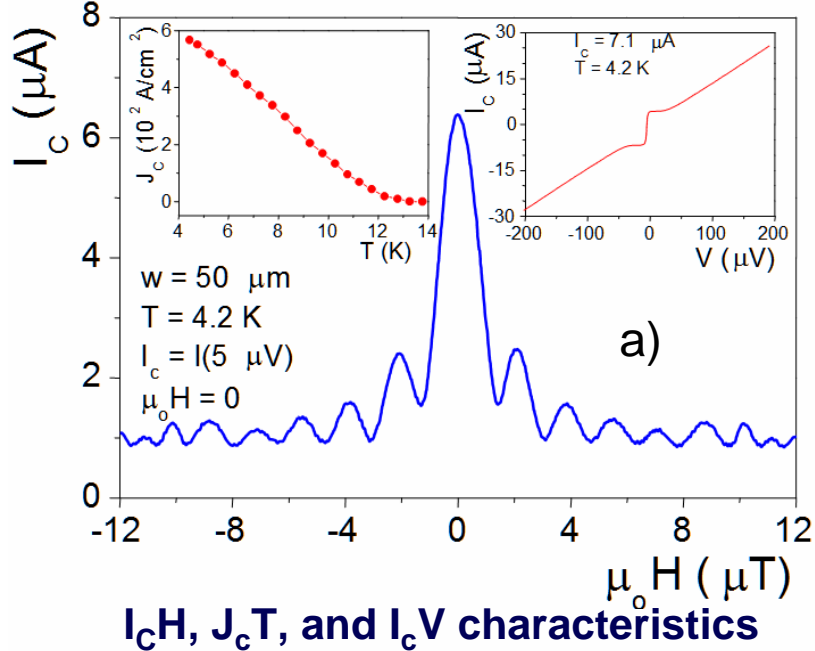
Tomaschko, Leca, Selistrovski,
Kleiner, Koelle, Phys. Rev. B 84 (2011)

$Sr_{1-x}La_xCuO_2$ 24° symmetric grain boundary junctions

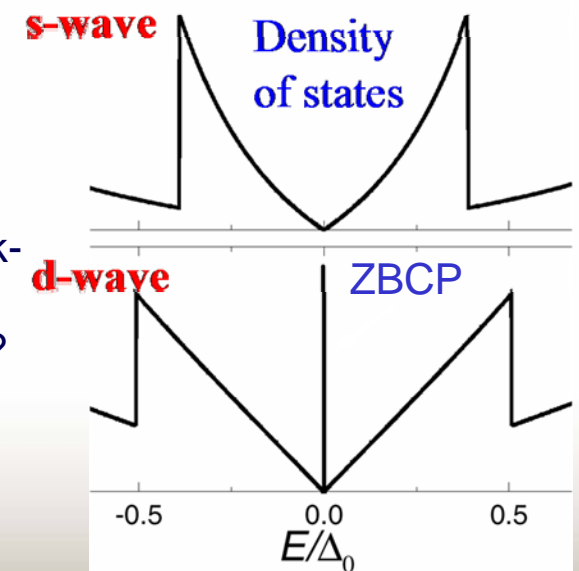
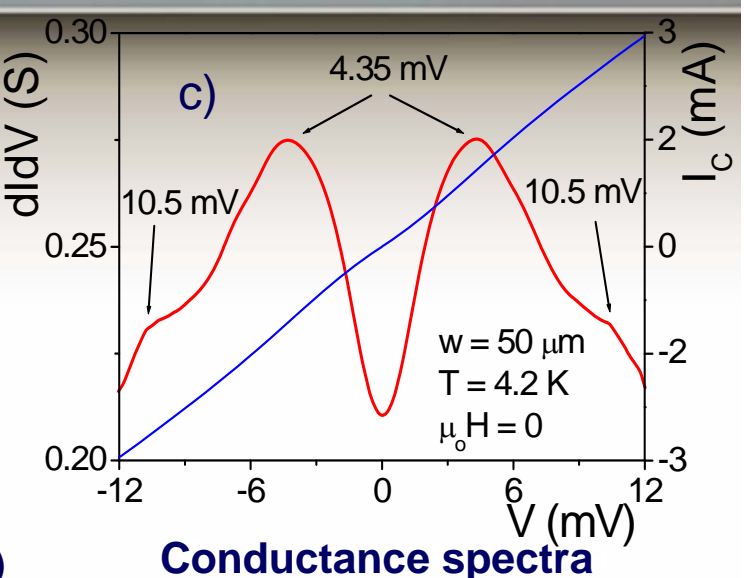
Microstructure



$\text{Sr}_{1-x}\text{La}_x\text{CuO}_2$ 30° symmetric grain boundary junctions



HRSTEM image
(SrTiO_3 bicrystal)



a) I_cVs : resistively and capacitively shunted junction (RCSJ)-like;

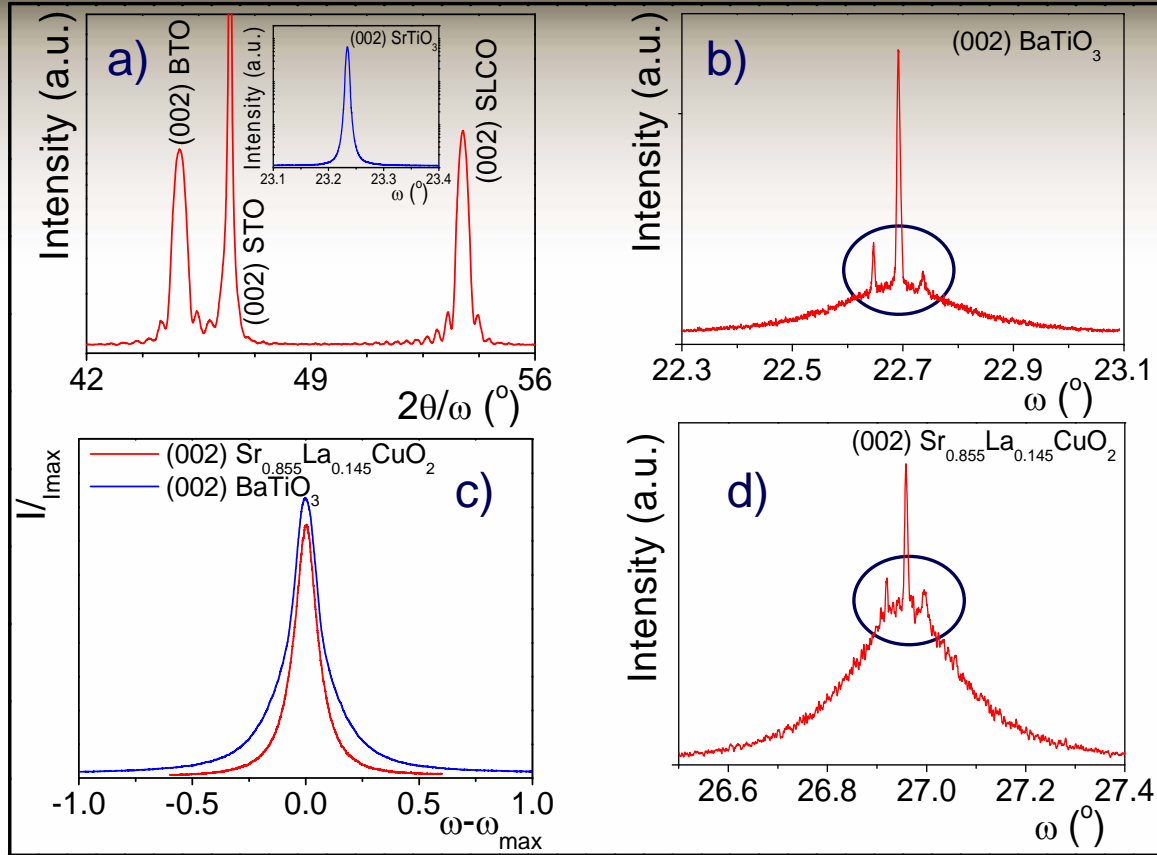
- highly regular Fraunhofer-like patterns;

- high J_c @ 4.2 K of $\sim 0.55 \text{ kA/cm}^2$; $I_c R_n$ of $\sim 50 \mu\text{V}$

b) conductance spectra did not show a zero-bias conductance peak-ZBCP, but a V-shaped subgap spectra **and** extra peaks above the coherence peaks; microscopic roughness due to structural defects?

c) plain view HRTEM of the substrate (30°) grain boundary.

$\text{Sr}_{1-x}\text{La}_x\text{CuO}_2$ 30° symmetric grain boundary junctions



Microstructure

Misfit strain accommodation by lattice modulations
Two components in ω scans: strained and relaxed

lattice modulations visible *only* in the HRXRD scans

XRD (a,c) and HRXRD (b, d) data for BTO/SLCO films grown on 30° GB

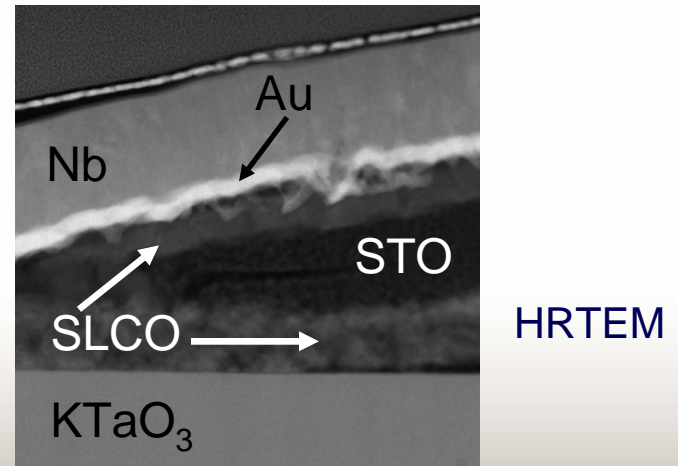
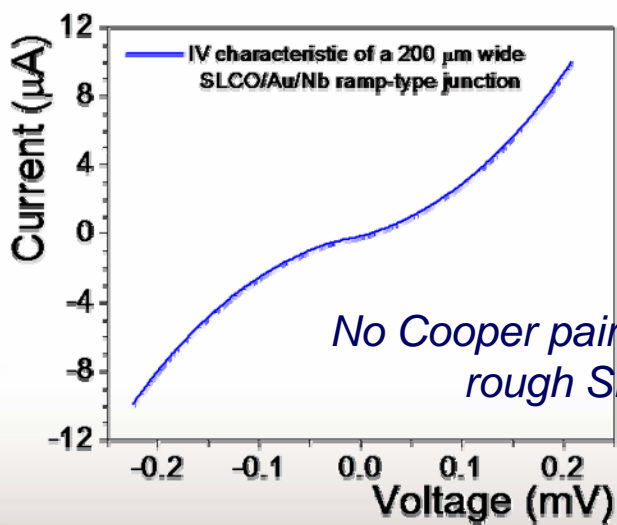
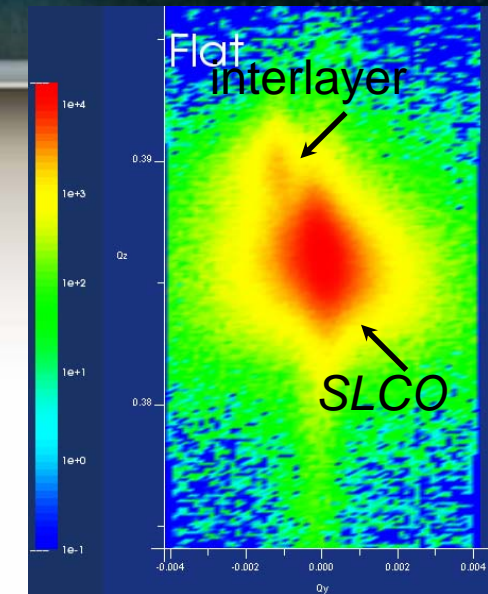
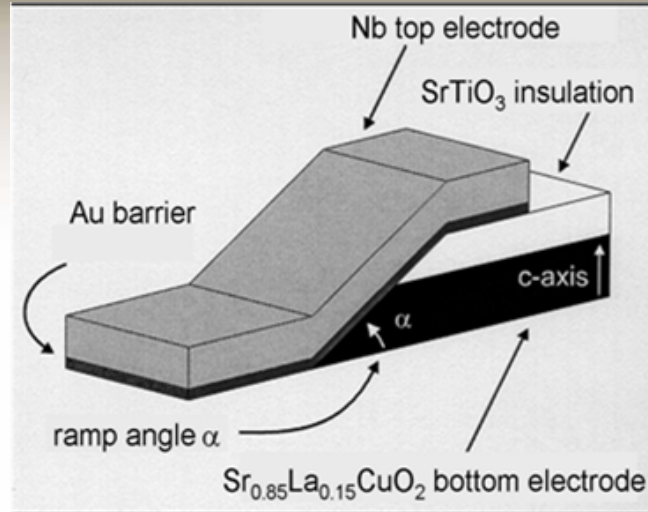
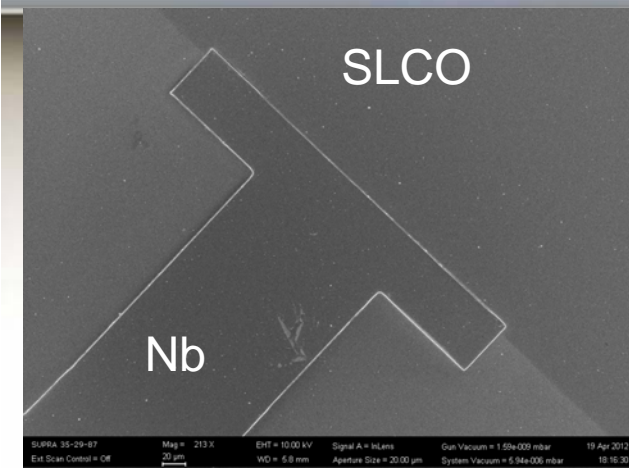
XRD scans in double (one monochromator) and triple (two monochromators) axes configuration showing the presence of dislocations in the (buffer) BaTiO₃ and SLCO layers.

HRXRD: triple axes configuration

XRD: double axes configuration

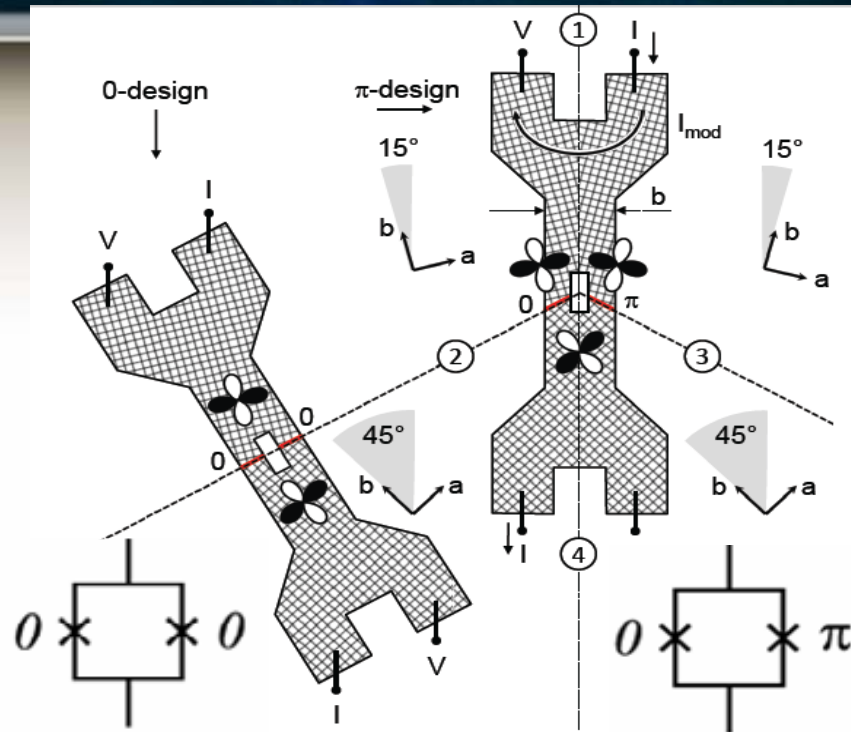
Leca, Tomaschko, Danila, Kleiner, Koelle, unpublished

$Sr_{1-x}La_xCuO_2$ ramp-type junctions



Phase sensitive experiments using π -SQUIDs

Pairing symmetry from phase sensitive experiments



Schematic layout of the
0 - and π -SQUIDs

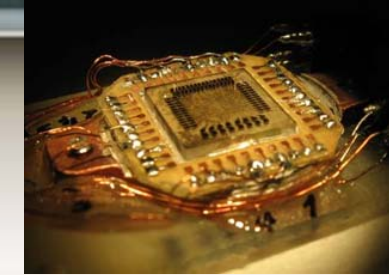
Geometry designed to be frustrated for d-wave pairing.

If d-wave: the dc-SQUID ring around the tetracrystal point contains one 0-junction and one π -junction (forming the π -SQUID, which exhibits an additional π shift in its phase).

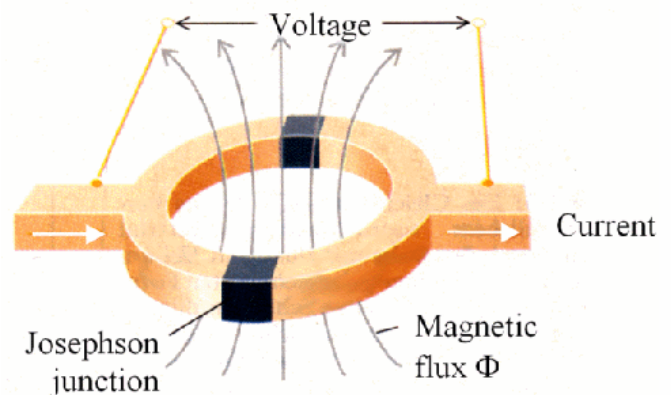
Phase-sensitive experiments rely on sign change in the Josephson I_c (a qualitative signature of unconventional Sc), and not on quantitative magnitude of the I_c .

Tsuei et al. RMP 72 (2000)

[Schulz et al., APL 76 (2000); Chesca et al., PRL 90 (2003)]

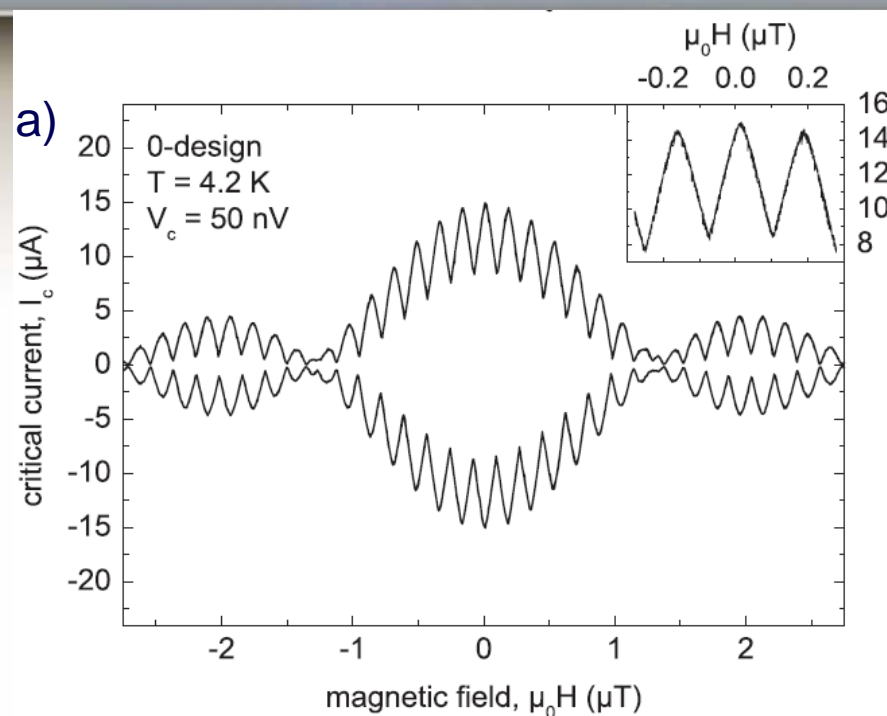


The SrTiO_3 tetracrystal
with structured SQUIDS

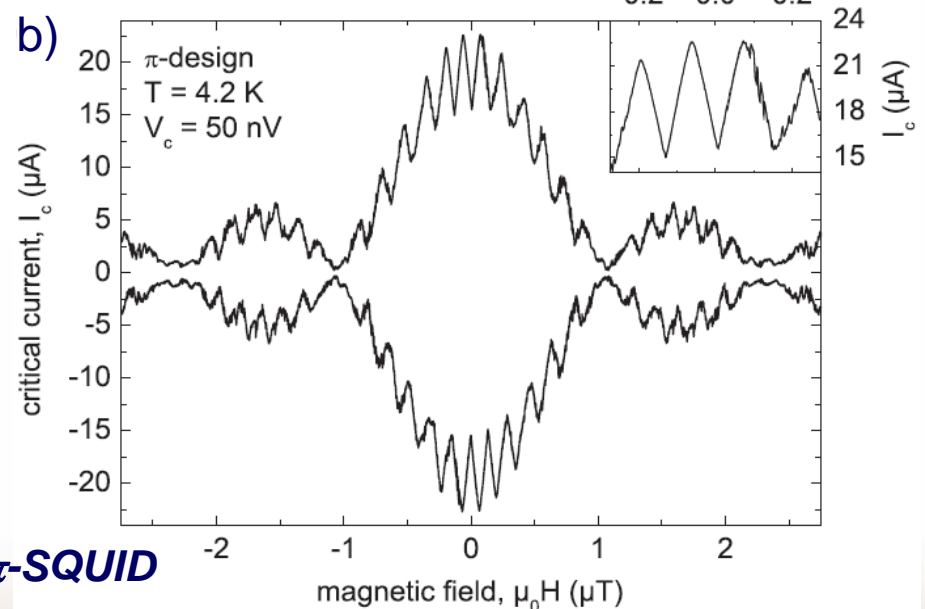
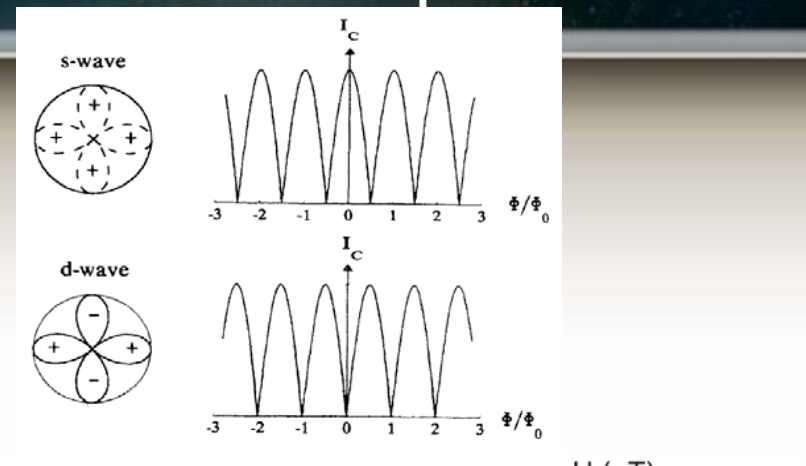


Design of a dc-SQUID

Pairing symmetry from phase sensitive experiments



I_c vs magnetic field for
a) 0 - and b) π -SQUID



The I_c vs. H shows a minimum at $H=0$ for the π -SQUID due to the phase shift across the π -junction.

Predominantly $d_{x^2-y^2}$ pairing symmetry

Tomaschko et al., Phys. Rev. B 86 (2012)

Conclusions

The superconducting properties of the PLD grown electron-doped $\text{Sr}_{1-x}\text{La}_x\text{CuO}_2$ thin films are still far of those of the bulk or of the MBE grown films; however, higher phase stability can be achieved by PLD (in the over doped region).

No zero bias conductance peak observed in grain-boundary junctions, most probably due to oxygen vacancies along the grain boundary.

Phase sensitive experiments shown a predominantly d-wave order parameter symmetry in the $\text{Sr}_{1-x}\text{La}_x\text{CuO}_2$ ($x \sim 0.15$) thin films.

